Kerbala Journal of Pharmaceutical Sciences

ISSN: 2221-7207(Print) / **ISSN**: 3006-7189 (Online)

Synthesis, in silico Biological and ADMET Predictions, and Molecular Docking of Isatin Schiff Base Derivatives as Promising Antituberculosis Agents

Meeqaat H. Altrufi[1*], Samer A. Hasan[1], Zeyad Kadhim Oleiwi[1]

[1]Department of Pharmaceutical Chemistry, College of Pharmacy, University of Kufa, Najaf

[*]**Corresponding author:**

Meeqat Hamid Alturfi: meeqaath.alturfi@student.uokufa.edu.iq

Received: 29/06/2025
Accepted: 19/08/2025
Published: 31/12/2025

Keywords: Isatin Schiff bases; Mycobacterium tuberculosis; antitubercular; InhA; molecular docking; ADMET.

DOI:10.62472/kjps.v16.i27.25-43

Abstract

Tuberculosis (TB), caused by *Mycobacterium tuberculosis*, continues to be a global health challenge, particularly with the rise of multidrug-resistant (MDR) and extensively drug-resistant (XDR) strains. In this study, five isatin Schiff base derivatives were designed, synthesized, and evaluated using *in silico* approaches to identify potential antitubercular agents. The ADMET profiles of isatin Schiff base derivatives were studied via pkCSM, admetSAR, and SwissADME servers. Biological activity predictions were conducted using the PASS online tool, with significant activity considered at Pa > 0.7. Molecular docking studies were performed using MOE software targeting the InhA enzyme (PDB ID: **4TZK**), a key protein in the fatty acid synthesis pathway of *Mycobacterium tuberculosis*. The docking results revealed that all five ligands exhibited favorable binding affinities and strong interactions with the enzyme's active site. Additionally, the ADMET profiles suggested good drug-likeness and acceptable pharmacokinetic behavior. These findings suggest that the synthesized isatin Schiff base derivatives **(A1–A5)** are promising candidates for further development as antitubercular agents. Conclusion: This study demonstrated that the five isatin Schiff base derivatives **(A1–A5)** show strong potential as antitubercular agents. Molecular docking revealed promising interactions with the InhA enzyme, especially for ligand **A5**. ADMET studies analyses further supported their drug-likeness and biological activity. These findings warrant further experimental validation and optimization.

التخليق ، والالتحام الجزيئي لمشتقات (ADMET) تخليق، وتنبؤات بيولوجية ودوائية حاسوبية "شيف للإيزاتين كعوامل واعدة مضادة لمرض السل

ميقات حامد اعوج، سامر علي حسن، زياد كاظم عليوي

السل الذي تسببه بكتيريا *Mycobacterium tuberculosis*، لا يزال يمثل تحديًا صحيًا عالميًا، خاصة مع تزايد حالات السل المقاوم للأدوية المتعددة (MDR) والسل شديد المقاومة للأدوية .(XDR) في هذه الدراسة، تم تصميم وتخليق خمسة مشتقات شيف من الإيزاتين، وتقييمها باستخدام أساليب حوسبية (in silico) لتحديد مدى إمكانيتها كمضادات للسل. تم تحليل الخصائص الدوائية والتسممية (ADMET) لهذه المشتقات باستخدام مواقع pkCSM و admetSARو .SwissADMEكما تم التنبؤ بالنشاط البيولوجي باستخدام أداة PASS الإلكترونية، حيث اعتُبر النشاط ملحوظًا عند قيمة احتمال (Pa) أكبر من 0.7 تم إجراء دراسات الالتحام الجزيئي باستخدام برنامج MOE مستهدفين إنزيم) InhA رمز(PDB: 4TZK ، وهو إنزيم رئيسي في مسار تخليق الأحماض الدهنية في *Mycobacterium tuberculosis*.أظهرت نتائج الالتحام أن جميع المركبات الخمسة أبدت تقاربات ارتباط جيدة وتفاعلات قوية مع الموقع النشط للإنزيم. بالإضافة إلى ذلك، أشارت تحاليل ADMET إلى امتلاك المركبات خصائص دوائية مقبولة وقابلية جيدة للتطوير كعقاقير. **الاستنتاج :**أظهرت هذه الدراسة أن مشتقات شيف من الإيزاتين الخمسة (A1–A5)تمتلك قدرة واعدة كمضادات للسل. وقد أظهر الالتحام الجزيئي تفاعلات قوية مع إنزيمInhA ، لا سيما المركب .A5 كما دعمت تحاليل ADMET قابلية هذه المركبات للتطور كأدوية ونشاطها البيولوجي. وتشير هذه النتائج إلى ضرورة إجراء دراسات تجريبية إضافية لتأكيد هذه النتائج وتحسين المركبات.

1. Introduction

Tuberculosis (TB) is a chronic infectious disease caused primarily by the bacterium *Mycobacterium tuberculosis*. It most commonly affects the lungs (pulmonary TB) but can also involve other organs such as the brain, kidneys, and spine (extrapulmonary TB). TB is transmitted through airborne droplets when an infected person coughs, sneezes, or speaks (Patel et al., 2025)**.** Despite being preventable and treatable, TB remains one of the top 10 causes of death worldwide. According to the World Health Organization (WHO), nearly 10 million people develop active TB each year, and around 1.3 million deaths occur annually due to the disease. TB can present with symptoms such as persistent cough, weight loss, night sweats, and fever. However, some individuals may carry a latent TB infection, show no symptoms, but still harbor the bacteria(Khattak et al., 2024). The emergence of multidrug-resistant TB (MDR-TB) and extensively drug-resistant TB (XDR-TB) has posed significant challenges to global TB control. These resistant strains do not respond to standard first-line anti-TB drugs, requiring longer and more complex treatment regimens. Effective TB management includes early diagnosis, proper antibiotic treatment, vaccination with BCG (Bacillus Calmette–Guérin), and public health measures to prevent transmission. Research into novel drugs, including natural and synthetic ligands, is critical to combat resistance and improve therapeutic outcomes(Pal et al., 2025, Nyang'wa et al., 2024). Anti-tubercular drugs recommended for treating tuberculosis include rifampicin, pyrazinamide, para-amino -salicylic acid, and isoniazid(Adeniji et al., 2020). Isatin (1H-indole-2,3-dione) is a naturally occurring compound found in plants, animals, and microorganisms. It has become an important pharmacophore in medicinal chemistry due to its wide range of biological activities(Nazir and Naseer, 2025)**.** Schiff bases are versatile ligands formed by the condensation of primary amines with aldehydes or ketones, resulting in an imine (-C=N-) functional group. These ligands exhibit a wide range of pharmacological activities, including antibacterial, antifungal, anticancer, and antitubercular effects. Their ability to interact with biological targets through hydrogen bonding and coordination enhances their therapeutic potential(Chowdhary et al., 2022) **.** In the present study, isatin Schiff base derivatives (**A1**–**A5**) were synthesized, combining the ADMET, biological activity and toxicological predictions. These ligands were evaluated using in silico tools and demonstrated promising binding affinity toward the InhA protein of Mycobacterium tuberculosis, suggesting their potential as lead antitubercular agents. Isatin derivatives have shown significant antimicrobial effects, including antibacterial and antifungal properties. Some ligands are particularly active against Mycobacterium tuberculosis, making them promising antituberculosis agents. These derivatives can inhibit key bacterial enzymes such as enoyl-ACP reductase (InhA) and DNA gyrase(Revuelta-Maza et al., 2020). In addition to their antimicrobial activity, isatin derivatives exhibit potent anticancer effects by promoting apoptosis and inhibiting tumor cell proliferation. Certain isatin ligands also display antiviral activity against HIV and herpes viruses. Moreover, they have demonstrated antioxidant properties by scavenging harmful free radicals. Several isatin analogues act as anti-inflammatory agents by modulating cytokine release **(Thorat et al., 2013).** Others possess anticonvulsant and antidepressant potential due to interactions with neurological targets. The versatility of the isatin scaffold allows structural modifications that can enhance selectivity and potency. Consequently, isatin-based ligands are considered

promising candidates in drug discovery and therapeutic development across multiple disease areas(Lagunin et al., 2000, Pires et al., 2015) **.**

2. Materials and Methods

2.1. Obtaining the Molecular Structures and The SMILE Via Chemdraw 20.0

The molecular structures of five isatin Schiff base derivatives**(A1-A5)** were sketched in ChemDraw 20.0 software to obtain the SMILEs Table1 of these structures that allow the subsequent analyses, Table1.

Table1: Obtaining the molecular structures and the SMILE via ChemDraw 20.0

Comp.	IUPAC name	Molecular Structure	SMILEs
A1	(Z)-3,4,5-trimethoxy-N'-(2-oxoindolin-3-ylidene) benzohydrazide	O=C(N/N=C1C(NC2=C\1C=CC=C2)=O)C3=CC(OC)=C(OC)C(OC)=C3	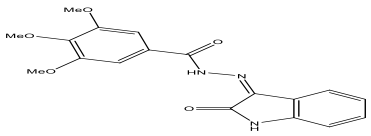
A2	(Z)-N'-(5-fluoro-2-oxoindolin-3-ylidene)-3,4,5-trimethoxybenzohydrazide	O=C(N/N=C1C(NC2=C\1C=C(F)C=C2)=O)C3=CC(OC)=C(OC)C(OC)=C3	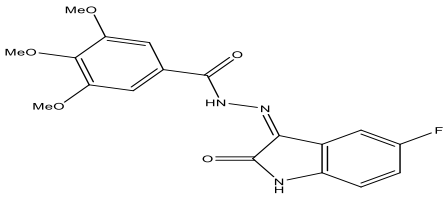
A3	(Z)-3,4,5-trimethoxy-N'-(5-methyl-2-oxoindolin-3-ylidene) benzohydrazide	Fc1cc2/C(=N/NC(=O)c3cc(OC)c(OC)c(OC)c3)/C(=O)Nc2cc1	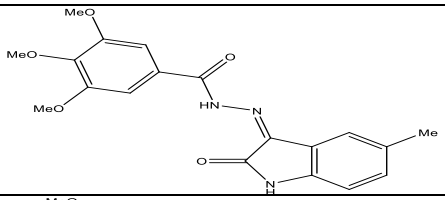
A4	(Z)-3,4,5-trimethoxy-N'-(5-nitro -2-oxoindolin-3-ylidene) benzohydrazide	O=C(N/N=C/1\C(=O)Nc2c\1cc(C)cc2)c1cc(OC)c(OC)c(OC)c1	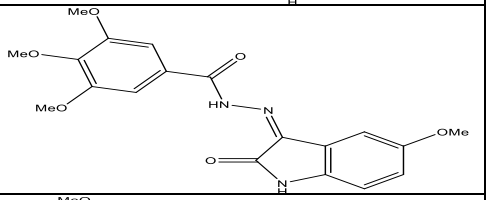
A5	(Z)-3,4,5-trimethoxy-N'-(5-methoxy-2-oxoindolin-3-ylidene) benzohydrazide	O=[N+]([O])c1cc2/C(=N/NC(=O)c3cc(OC)c(OC)c(OC)c3)/C(=O)Nc2cc1	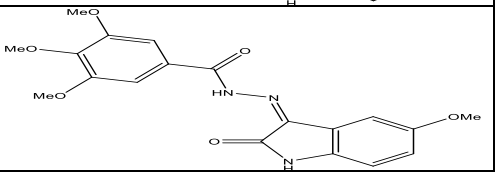

2.2. Prediction of ADMET Profile Using Pkcsm, Admetsar And Swissadme Web Servers in Combination

The web servers PKCSM—Predicting Small-Molecule Pharmacokinetic and Toxicity Properties Using Graph-Based Signatures (https://biosig.lab.uq.edu.au/pkcsm/), admetSAR-ADMET structure-activity relationship database (http://lmmd.ecust.edu.cn/admetsar2), and SwissADME (http://www.swissadme.ch/) of the Swiss Institute of Bioinformatics provide predictions about pharmacokinetic processes (absorption, distribution, metabolism, excretion, and toxicity) of drug candidates from their SMILE(Banerjee et al., 2018).

2.3. WAY2Drug to Predict Biological Activities

WAY2Drug (http://www.way2drug.com/PASSOnline/index.php) is an informational-computational platform capable of predicting the biological activity of drug-like compounds. This web base uses more than 250,000 biologically active structures to predict the potential physical activity using the SMILE of the molecules. The viability of a particular spectrum of biological activity is given by Pa (probability "to be active") and Pi (probability "to be inactive"). In this case, Pa > 0.7 was used. Notably, the values of Pa and Pi are more closely related to the similarity with the training set of the platform and usually have no direct relationship with the quantitative characteristics of the activity(Pagadala et al., 2017) **.**

2.4. Protox-II to Predict Toxicity

The endpoints toxicity (hepatotoxicity, neurotoxicity, nephrotoxicity, and cardiotoxicity) and organ toxicity (carcinogenicity, immunotoxicity, mutagenicity, and cytotoxicity) for the Isatin Schiff base derivatives (**A1-A5**), in addition to the LD_{50} of them, were calculated using the online software ProTox-II (https://tox-new.charite.de/protox_II/)(Meng et al., 2011) **.**

2.5. Molecular Docking

Molecular docking is widely used to provide the possible binding conformations of the chemical compounds in a receptor(Furniss, 2004). This study was performed to find interactions between the ligands under investigation and the active site residues of the selected protein, to compare binding affinities and RMSD values between them, and to evaluate the best conformers based on the lowest binding affinities. Molecular docking of the identified receptor and all of the ligands was carried out using Molecular Operating Environment (MOE) software 2024.06(Hossain and Zakaria, 2017) **.**

The X-ray crystal coordinate of the crystal structure of *Mycobacterium tuberculosis* enoyl reductase (INHA) (PDB ID: 4TZK), as shown in Fig.1 and Table2, with a high resolution of 1.62 Å, was downloaded from the RCSB database (http://www.rcsb.org/pdb), which is in the bound state with co-crystallized ligand **641**. The molecular structure of co-crystallized ligand **(641)**, which is shown in Figure 2. The docking process involves two steps.

2.6. Ligand Preparation:

All previously sketched molecular structures of five isatin base derivatives (**A1-A5**) have undergone energy minimization and conformational analysis of molecules (level: ultra) employing Chem3D Pro 19.1 software by means of the Molecular Mechanics Force Field (MM+), like MM2 and then MMFF94. The reduction process is repeated until the root mean square (RMS) gradient value falls below 0.1 kcal/mol. After that, in MOE, protonating the ligand in 3D shape, partial charge addition, energy minimization, and finally saving the results.

2.7. Protein preparation:

The downloaded crystal structure of the crystal structure of *Mycobacterium tuberculosis* enoyl reductase (INHA) (PDB ID: 4TZK) has been prepared through the following steps: The chain sequences that participate in the protein action were only selected. The small molecules and only unnecessary water molecules were removed. Adding hydrogen hides bonds; after that, fix the potential of the protein atoms and identify its active sites. At the end, all the previously prepared ligands were loaded into MOE from saved data, followed by the docking process along with co-crystallized ligand 4TZK for comparative study. The pose with a higher

binding affinity (less S score) and proper RMSD value (less than 2) was selected. Table 11 illustrates the binding affinities and RMSD values of the selected poses of ligands, as well as the types of interactions, bond distances (Å), and bonding energies E (kcal/mol) between involved atoms of all ligands and atoms of the involved residues of the identified active site of the 4TZK protein, Table2 and Fig.1 A-B.

Table2: Information Details Related to The Protein 4ZTK.

Protein	Method	Resolution (Å)	Amino acid number	Atom Count	Total Structure Weight	Organism	Co-crystalized ligand (AQ4)	Docking Score	RMSD
4TZK	X-ray diffraction	1.62	269	2,432	29.57 kDa	*Mycobacterium tuberculosis* H37Rv	1-Cyclohexyl-N-(3,5-dichlorophenyl) -5-oxopyrrolidine-3-carboxamide (Pyrrolidine carboxamide)	-7.01	0.847

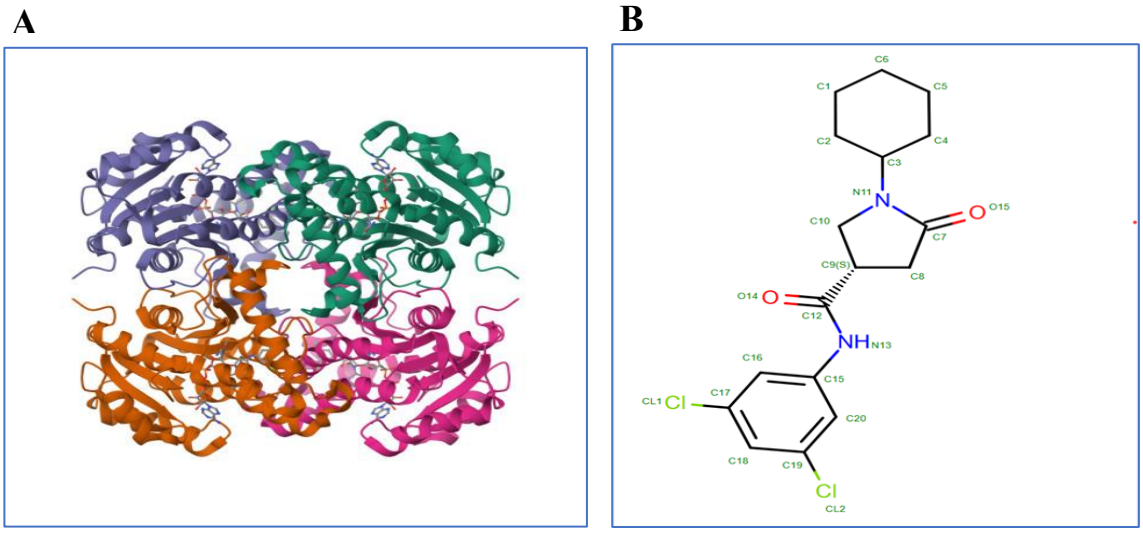

Figure1: A) Crystal structure of Mycobacterium tuberculosis enoyl reductase **(INHA) (PDB ID: 4TZK). B)** Chemical structure of co- crystalized ligand 641

2.8. Synthesis of isatin Schiff base derivatives (A1-A5)

2.8.1. General procedure for the synthesis of Methyl 3,4,5-trimethoxybenzoate (1)

Add to 50 mL round-bottom flask, 0.0235 mol (5 g) of trimethoxybenzoic acid was dissolved in 25 mL of methanol. Then, 1 mL of concentrated sulfuric acid was added as a catalyst. The reaction mixture was heated under reflux for 8 hours to promote Fischer esterification (Hussein et al., 2023). After completion, the mixture was cooled and poured over 20 g of crushed ice. The resulting precipitate was filtered, washed with cold water, and recrystallized from absolute ethanol to obtain compound (1) in pure form.

2.8.2. General procedure for the synthesis of 3,4,5-trimethoxybenzohydrazide (2)

Compound1 (0.0221 mol ,4.06 g) was reacted with an excess of hydrazine hydrate 80% (0.08 mol, 5 mL) in 50 mL of absolute ethanol. The reaction mixture was refluxed at 80 °C for 12 hours in a 100 mL round-bottom flask (Hussein et al., 2023)**.** Upon cooling, the solid product was collected by filtration, washed with ethanol, and dried. Recrystallization from 90% ethanol yielded the hydrazide (Compound2).

2.8.3. General procedure for the synthesis of isatin Schiff base derivatives (A1–A5) (Hussein et al., 2023)washed with ethanol and diethyl ether, and recrystallized from ethanol. The final products (**A1–A5**) were dried at room temperature, as presented in Fig.2.

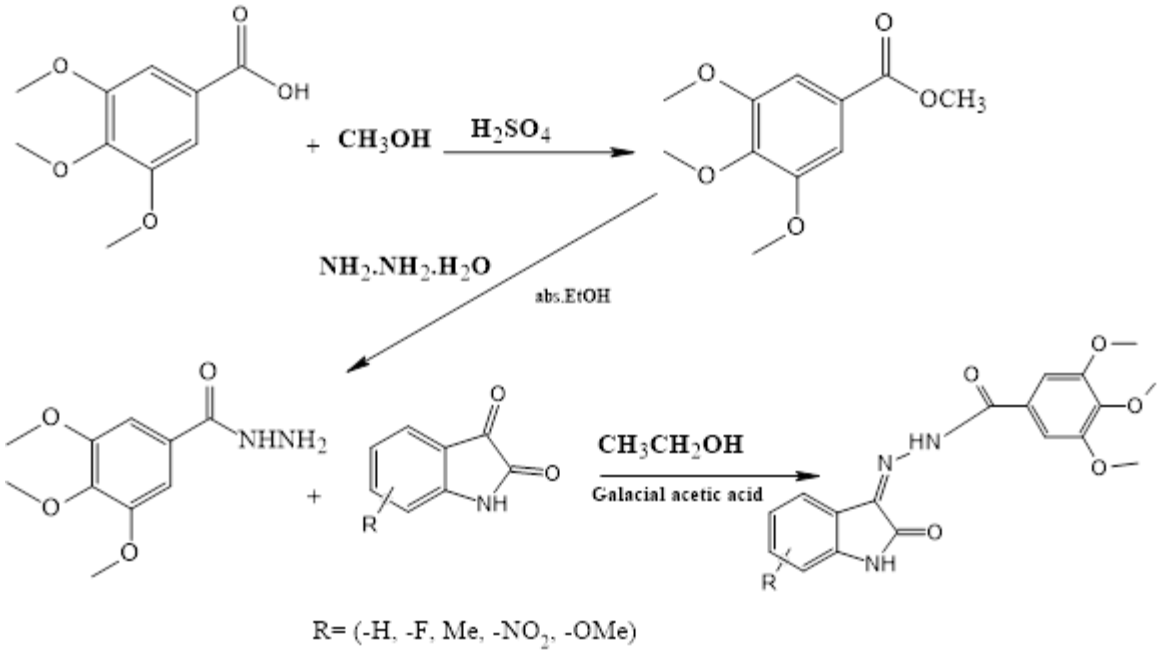

Figure2: Synthetic Scheme for The Synthesis of Isatin Schiff Base Derivatives (A1-A5)

3. Results

3.1. Initial Information About the Isatin Schiff Base Derivatives (A1-A5)

As mentioned previously, the molecular structures of the isatin Schiff bases (**A1-A5**) were sketched in ChemDraw 20.0 to obtain the SMILEs (Table 1). Therefore, a compound with drug-like properties must have specific criteria, which include less than 10 H-bond acceptors and less than 5 H-bond donors; a molecular weight not greater than 500 gm/mol; and logP, with a value below 5, not being able to violate more than one of these parameters (Hamada and Kiso, 2017)**.** Additionally, to consider the permeability and flexibility, the polar surface area must be equal to or less than 140 and have no more than 10 rotational bonds, in that order (Case et al., 2023)**.** Still, the molecular volume is the feature that can determine factors such as intestinal absorption and blood-brain barrier penetration. All the isatin Schiff base derivatives **(A1-A5)** complied, exhibiting favorable pharmacokinetic properties.

3.2. Prediction of ADMET Profile Using Pkcsm, Admetsar, And Swissadme Servers In Combination

The five ligands (**A1–A5**) demonstrated notable differences in their physicochemical and pharmacokinetic profiles, which may impact their drug-likeness and bioavailability. In terms of water solubility, all compounds exhibited relatively poor solubility (log mol/L < -3), with **A5** being the least soluble (-4.637), potentially due to its higher hydrophobic character. Caco-2 permeability data showed **A5** had the highest permeability (1.264 log Papp), indicating better intestinal absorption potential, which aligns with its highest predicted human intestinal absorption (95.36%). Notably, all ligands except **A5** were identified as P-glycoprotein substrates and inhibitors, suggesting possible efflux-related bioavailability limitations. Conversely, **A5** avoided P-gp interaction, which might explain its superior absorption metrics. Skin permeability (log Kp) was relatively consistent across all ligands, with slightly higher skin penetration potential observed for **A3**. Regarding CYP450 interactions, **A1–A4** were identified as substrates for CYP3A4 and inhibitors for multiple isoforms, reflecting potential metabolic instability or drug–drug interaction risks. **A5**, in contrast, was a non-substrate for most enzymes, possibly indicating lower metabolic liability. From a physicochemical standpoint, **A4** had the highest surface area and molecular weight, which may explain its lower gastrointestinal absorption prediction. Furthermore, **A5** showed the most favorable blood-brain barrier permeability and a balanced TPSA (107.48 Å²), indicating a potential for central nervous system activity. Overall, **A5** appears to be the most promising candidate among the group in terms of absorption and metabolic profile, likely due to its favorable permeability, lack of P-gp interaction, and minimal CYP inhibition, despite its lower solubility. These findings support its potential for further development, provided solubility can be enhanced via formulation strategies, presented in Table2, Table3 and Table4.

Table2: Prediction of ADMET Profiles of Isatin Schiff Base Derivatives (A1-A5) In the Webserver Pkcsm

Comp.		A1	A2	A3	A4	A5
Absorption	Water solubility (log mol/L)	-3.802	-4.111	-3.606	-3.829	-4.637
	Caco2, permeability, (log Papp in 10^{-6} cm/s)	0.373	1.134	0.876	1.207	1.264
	Intestinal absorption (human) (% Absorbed)	77.141	69.485	77.089	73.554	95.359
	Skin, Permeability, (log Kp)	-2.991	-2.942	-2.813	-2.863	-2.872
	P-glycoprotein substrate (Yes/No)	Yes	Yes	Yes	Yes	NO
	P-glycoprotein I, inhibitor (Yes/No)	Yes	Yes	Yes	Yes	NO
	P-glycoprotein, II inhibitor (Yes/No)	NO	NO	NO	NO	NO
Molecule properties	Descriptor					
	Molecular Weight	355.35	373.34	369.38	872.34	385.35
	LogP	1.9377	1.9377	1.7068	1.8072	316.353
	#Rotatable Bonds	5	5	6	6	6
	#Acceptors	6	6	8	7	5
	#Donors	2	2	2	2	1
	Surface Area (Å²)	153.467	153.467	163.954	160.780	135.237

Table3: The Output Parameters of Drug-Likeness and ADME For Isatin Schiff Base Derivatives (A1-A5) In the Webserver Admetsar

Comp.	Model	Result	Probability
A1	**Absorption**		
	Metabolism		
	CYP450, 2C9 Substrate.	Non-substrate	0.8286
	CYP450 ,2D6 Substrate.	Non-substrate	0.8447
	CYP450 ,3A4 Substrate.	Substrate	0.6161
	CYP450, 1A2 Inhibitor.	Inhibitor	0.6542
	CYP450 ,2C9 Inhibitor.	Inhibitor	0.6928
	CYP450 ,2D6 Inhibitor.	Non-inhibitor	0.9075
	CYP450 ,2C19 Inhibitor.	Non-inhibitor	0.5476
	CYP450 ,3A4 Inhibitor.	Non-inhibitor	0.6234
	CYP Inhibitory, Promiscuity.	High CYP Inhibitory Promiscuity	0.9013
A2	**Absorption**		
	Blood-Brain, Barrier.	BBB+	0.6397
	Human Intestinal Absorption	HIA+	0.9545
	Caco-2, Permeability	Caco2-	0.5706
	P-glycoprotein ,Substrate	Non-substrate	0.5203
	P-glycoprotein, Inhibitor	Non-inhibitor	0.5333
	Inhibitor,	0.6807	
	Renal Organic ,Cation Transporter	Non-inhibitor	0.8869
	Metabolism		
	CYP450 2C9, Substrate.	Non-substrate	0.7861
	CYP450 2D6, Substrate.	Non-substrate	0.8543
	CYP450 3A4 ,Substrate.	Substrate	0.6111
	CYP450 1A2 ,Inhibitor.	Inhibitor	0.6434
	CYP450, 2C9, Inhibitor.	Inhibitor	0.6515
	CYP450 2D6 ,Inhibitor	Non-inhibitor	0.9129
	CYP450 2C19 .Inhibitor,	Non-inhibitor	0.5939
	CYP450 3A4 Inhibitor,	Non-inhibitor	0.5603
	CYP Inhibitory ,Promiscuity.	High CYP Inhibitory Promiscuity	0.8559
A3	**Absorption**		
	Blood-Brain, Barrier.	BBB+	0.5088
	Human, Intestinal Absorption	HIA+	0.8305
	Caco-2, Permeability,	Caco2-	0.5605
	P-glycoprotein ,.Substrate,	Non-substrate	0.5361
	P-glycoprotein, Inhibitor.	Non-inhibitor	0.6641
	Inhibitor,	0.6164	
	Renal., Organic, Cation Transporter,.	Non-inhibitor	0.9067
	Blood-Brain Barrier		
	Human, Intestinal, Absorption,	HIA+	0.8305
	Caco-2 ,Permeability.	Caco2-	0.5605
	CYP450 ,2C9 Substrate.	Non-substrate	0.7470
	CYP450, 2D6 Substrate.	Non-substrate	0.8388
	CYP450 ,3A4 Substrate,	Substrate	0.6475
	CYP450, 1A2 Inhibitor.	Inhibitor	0.6799
	CYP450 2C9 Inhibitor.	Inhibitor	0.6655
	CYP450 ,2D6 ,Inhibitor.	Non-inhibitor	0.9075
	CYP450 2C19, Inhibitor.	Non-inhibitor	0.5967
A4	**Absorption**		
	Blood-Brain ,Barrier.	BBB+	0.6397
	Humans Intestinals mAbsorption	HIA+	0.9545

	Caco-2 Permeability,	Caco2-	0.5706
	P-glycoproteins Substrates.	Non-substrate	0.5203
	P-glycoproteins Inhibitors	Non-inhibitor	0.5333
	Inhibitors.	0.6807	
	Rena,l Organic Cations Transportesr	Non-inhibitor	0.8869
	Metabolism		
	CYP450s 2C9, Substrates	Non-substrate	0.7861
	CYP450, 2D6, Substrates	Non-substrate	0.8543
	CYP450 3A4 Substrates.	Substrate	0.6111
	CYP450 ,1A2 ,Inhibitors	Inhibitor	0.6434
	CYP450 2C9 Inhibitors.	Inhibitor	0.6515
	CYP450, 2D6, Inhibitor.	Non-inhibitor	0.9129
	CYP450 2C19, Inhibitor,	Non-inhibitor	0.5939
	CYP450, 3A4 Inhibitor.	Non-inhibitor	0.5603
	CYP, Inhibitory, Promiscuity.	High CYP Inhibitory Promiscuity	0.8559
A5	**Absorption**		
	Blood-Brain ,Barrier.	BBB+	0.8526
	Humans Intestinals Absorptions	HIA+	0.9882
	Caco-2 .Permeabilitys	Caco2+	0.8649
	P-glycoprotein,. Substrates	Non-substrate	0.5840
	P-glycoprotein, sInhibitor	Inhibitor	0.5659
	Non-inhibitor	0.5824	
	Renal Organic, Cation Transporter.	Non-inhibitor	0.8711
	Metabolism		
	CYP450 2C9, Substrates	Non-substrate	0.7321
	CYP450 2D6 Substrates	Non-substrate	0.7742
	CYP450, 3A4, Substrates	Non-substrate	0.5094
	CYP450, 1A2 Inhibitors.	Inhibitor	0.6781
	CYP450 2C9, Inhibitor.	Non-inhibitor	0.9658
	CYP450 2D6 Inhibitor	Non-inhibitor	0.8911
	CYP450 ,2C19 Inhibitor	Non-inhibitor	0.5529
	CYP450 3A4, Inhibitors,	Non-inhibitor	0.5175
	CYP Inhibitory. Promiscuity.	High CYP Inhibitory Promiscuity	0.7126

Table4: Prediction of ADMET Profiles of Isatin Schiff Base Derivatives (A1-A5) Using Swissadme Platform

Comp.	MW (g/mol)	nRB	nHBA	nHBD	MR (m^3/mol)	TPSA (Å²)	iLOGP	GI Absorption	BBB permeant	P-gp	BS	Ro5
A1	355.34	6	6	2	97.41	98.25	2.63	High	No	No	0.55	Yes
A2	373.34	6	7	2	97.37	98.25	2.62	High	No	No	0.55	Yes
A3	369.37	6	6	2	102.38	98.25	2.85	High	No	No	0.55	Yes
A4	400.34	7	8	2	106.23	144.07	2.05	Low	No	Yes	0.55	Yes
A5	385.37	7	7	2	103.9	107.48	2.86	High	No	Yes	0.55	Yes

3.3. WAY2Drug To Predicted Biological Activity

PASS prediction analysis revealed distinct differences in the biological potential of the five Isatin Schiff base derivatives (**A1–A5**). Ligand **A1** demonstrated notable predicted activities, acting as an amine dehydrogenase inhibitor (Pa = 0.745), antitubercular agent (Pa = 0.738), and antimycobacterial compound (Pa = 0.729), indicating a promising profile against mycobacterial infections. In contrast, ligand **A2** exhibited no significant predicted activity in the tested categories, suggesting minimal pharmacological potential. Ligand **A3** showed selective but potent action with antitubercular (Pa = 0.744) and antimycobacterial (Pa = 0.741) effects. Among all ligands, **A4** achieved the highest predicted values, with a Pa of 0.821 for antitubercular activity and 0.811 for antimycobacterial activity, highlighting its strong potential as an anti-TB candidate. Ligand **A5** displayed a diverse range of activities, including inhibition of amine dehydrogenase (Pa = 0.774), antitubercular (Pa = 0.721), antimycobacterial (Pa = 0.713), and gluconate 2-dehydrogenase (Pa = 0.713), suggesting its utility as a multitarget agent with antimicrobial potential, as shown in Table5.

Table5: The Biological Activities Prediction of The Isatin Schiff Bases Derivatives (A1_A2) In the Way2Drug Pass Online Tool

Comp.	Activity	Pa	pi
A1	Amine dehydrogenase inhibitor	0,745	0,005
	Antituberculosic	0,738	0,004
	Antimycobacterial	0,729	0,005
A2	-	-	-
A3	Antituberculosic	0,744	0,004
	Antimycobacterial	0,741	0,005
A4	Antituberculosic	0,821	0,003
	Antimycobacterial	0,811	0,004
A5	Amine dehydrogenase inhibitor	0,774	0,005
	Antituberculosic	0,721	0,004
	Antimycobacterial	0,713	0,005
	Gluconate 2-dehydrogenase (acceptor) inhibitor	0,713	0,049

3.3. The Predict Toxicity Results and LD50 (Mg/Kg) Of Isatin Schiff Base Derivatives (A1-A5).

The in-silico toxicity analysis of ligands **A1** through **A5** revealed consistent patterns across all tested molecules. All five ligands are classified as Practically Non-Toxic (Toxicity Class 4), indicating a relatively safe toxicity profile based on general acute toxicity classification. None of the ligands showed nephrotoxicity or cardiotoxicity potential, with high confidence scores (0.90 and 0.77 respectively), suggesting they are unlikely to affect kidney or heart function adversely. However, a common concern across all compounds is the predicted hepatotoxicity (DILI) and neurotoxicity, both identified as *active* with high probabilities (0.69 for DILI and 0.87 for neurotoxicity). This indicates a potential risk of liver and central nervous system toxicity that may require careful consideration in further preclinical testing. for broader toxicological endpoints, carcinogenicity, mutagenicity, and cytotoxicity were consistently predicted as *inactive* across all ligands with strong confidence (0.62–0.97), indicating low risk for DNA damage, cancer development, or non-specific cell toxicity. However, all ligands showed active immunotoxicity with a very high probability

(0.96), which might suggest the potential for immune system-related adverse effects or hypersensitivity reactions upon exposure.in conclusion, while the ligands show promising safety in terms of nephrotoxicity, cardiotoxicity, and mutagenic or carcinogenic potential, the predicted hepatotoxicity, neurotoxicity, and immunotoxicity warrant further in vitro and in vivo validation before any clinical application. The consistency in these predictions across all five ligands may reflect a shared structural alert or pharmacophore responsible for these effects., see Table6.

Table6: The predict toxicity results and LD50 (mg/kg) of isatin Schiff base derivatives (A1_A2)

Comp.	PredictLD50 (mg/kg)	Classification	Target	Shorthand	Prediction	Probability
A1	1190	Organ toxicity	Hepatotoxicity	dili	Active	0.69
			Neurotoxicity	neuro	Active	0.87
Practically Non-Toxic			Nephrotoxicity	nephro	Inactive	0.90
			Cardiotoxicity	cardio	Inactive	0.77
Predicted Toxicity Class: 4		Toxicity end points	Carcinogenicity	carcino	Inactive	0.62
			Immunotoxicity	immuno	Active	0.96
			Mutagenicity	mutagen	Inactive	0.97
			Cytotoxicity	cyto	Inactive	0.93
A2	1190	Organ toxicity	Hepatotoxicity	dili	Active	0.69
			Neurotoxicity	neuro	Active	0.87
Practically Non-Toxic			Nephrotoxicity	nephro	Inactive	0.90
			Cardiotoxicity	cardio	Inactive	0.77
Predicted Toxicity Class: 4		Toxicity end points	Carcinogenicity	carcino	Inactive	0.62
			Immunotoxicity	immuno	Active	0.96
			Mutagenicity	mutagen	Inactive	0.97
			Cytotoxicity	cyto	Inactive	0.93
A3	1190	Organ toxicity	Hepatotoxicity	dili	Active	0.69
			Neurotoxicity	neuro	Active	0.87
Practically Non-Toxic			Nephrotoxicity	nephro	Inactive	0.90
			Cardiotoxicity	cardio	Inactive	0.77
Predicted Toxicity Class:4		Toxicity end points	Carcinogenicity	carcino	Inactive	0.62
			Immunotoxicity	immuno	Active	0.96
			Mutagenicity	mutagen	Inactive	0.97
			Cytotoxicity	cyto	Inactive	0.93
A4	1190	Organ toxicity	Hepatotoxicity	dili	Active	0.69
			Neurotoxicity	neuro	Active	0.87
Practically Non-Toxic			Nephrotoxicity	nephro	Inactive	0.90
			Cardiotoxicity	cardio	Inactive	0.77
Predicted Toxicity Class: 4		Toxicity end points	Carcinogenicity	carcino	Inactive	0.62
			Immunotoxicity	immuno	Active	0.96
			Mutagenicity	mutagen	Inactive	0.97
			Cytotoxicity	cyto	Inactive	0.93
A5	1190	Organ toxicity	Hepatotoxicity	dili	Active	0.69
			Neurotoxicity	neuro	Active	0.87
Practically Non-Toxic 4			Nephrotoxicity	nephro	Inactive	0.90
			Cardiotoxicity	cardio	Inactive	0.77|
Predicted ToxiN		Toxicity end points	Carcinogenicity	carcino	Inactive	0.62
			Immunotoxicity	immuno	Active	0.96
			Mutagenicity	mutagen	Inactive	0.97
			Cytotoxicity	cyto	Inactive	0.93

3.4. Molecular Docking Results

The molecular docking study using MOE 2024.06 revealed that the isatin Schiff base derivatives (**A1**-**A5**) generally exhibited strong predicted binding affinities to the M. tuberculosis enoyl reductase (4TZK) active site, comparable to the co-crystallized ligand (**641**, S score = -7.017 kcal/mol). Notably, ligands **A3** (-7.167 kcal/mol) and **A4** (-7.234 kcal/mol) displayed slightly more favorable predicted binding energies than the reference co-crystallized ligand **(641), Table7**. Ligands **A1** (-6.860 kcal/mol), **A2** (-6.465 kcal/mol), and **A5** (-7.154 kcal/mol) also showed significant binding potential, though **A2** had the weakest affinity among the tested Schiff bases. demonstrate co-crystallized ligand **(641)** the most precise geometric fit within the binding site, as indicated by its low Root Mean Square Deviation (RMSD) of 0.847 Å. This suggests the docking protocol successfully reproduced the experimentally observed binding pose. In contrast, the Schiff base derivatives (**A1-A5)** showed higher RMSD values (ranging from 1.017 Å for A5 to 1.775 Å for A4), indicating their predicted binding modes deviate from the starting conformation used in docking. This is expected for compounds not originally crystallized in the site.The co-crystallized ligand **(641)** primarily formed hydrogen bonds: one as a donor (N13 atom to water HOH743, 2.91 Å, -2.7 kcal/mol) and one as an acceptor (O15 atom to TYR158 sidechain hydroxyl, 3.13 Å, -1.2 kcal/mol). This reliance on a water-mediated interaction and a single direct protein H-bond highlights a potentially less complex binding mode compared to some Schiff bases. The isatin Schiff base derivatives (**A1-A2**) engaged in a wider variety of interactions. MET199 (A) was a crucial residue, forming hydrophobic/H-donor interactions with **A1** (via C6, 3.98 Å, -0.8 kcal/mol) and **A3** (via C6 and N20). ASP148(A) acted as a key H-bond acceptor for **A2, A3,** and **A4** (via N12, distances ~3.00 Å, energies -1.1 to -2.0 kcal/mol). LYS165(A) formed a strong H-bond with **A2** (O15 acceptor to NZ, 2.77 Å, -3.1 kcal/mol). PHE149(A) consistently participated in stabilizing pi-H interactions with the aromatic rings of **A3, A4**, and **A5** (distances ~4.16 Å, energies ~-1.0 kcal/mol). Water-mediated H-bonds were also observed (A5, A3). while The co-crystallized ligand **(641)** relied on fewer direct protein interactions (mainly two H-bonds, one water-mediated), the Isatin Schiff base derivatives, particularly **A2, A3**, and **A5**, formed a richer network. **A2** and **A3** engaged in three H-bonds each, and **A5** combined two H-bonds (one water-mediated) with a pi-H interaction. **A3** and **A4** also utilized pi-H bonding with PHE149, an interaction type not seen with co-crystallized ligand **(641).** This suggests the Isatin Schiff bases exploit additional binding site features or form more numerous stabilizing contacts, potentially contributing to the strong S scores of **A3, A4,** and **A5** despite their higher RMSD values, Table8 and Fig.2.

Table7: Binding Site Residues of The Mycobacterium Tuberculosis Enoyl Reductase (PDB ID:4TZK)

Receptor	size	Recedes
4TZK	252	1:(SER13 GLY14 ILE15 ILE16 THR17 SER19 SER20 ILE21 ALA22 THR39 GLY40 PHE41 ASP42 ARG43 LEU46 ILE47 ILE50 LEU63 ASP64 VAL65 GLN66 SER94 ILE95 GLY96 PHE97 MET98 PRO99 GLN100 MET103 GLY104 LYS118 ILE122 MET147 ASP148 PHE149 MET155 PRO156 ALA157 TYR158 MET161 LYS165 ALA191 GLY192 PRO193 ILE194 THR196 LEU197 ALA198 MET199 ALA201 ILE202 ALA206 LEU207 ALA211 GLN214 ILE215 LEU218)

Table8: The Results Obtained from Docking of Ligands With 4TZK

Comp.	S score (kcal/mol)	RMSD (Å)	Atom of compound	Involved receptor atoms	Involved receptor residues	Type of interaction	Bond Distance (Å)	E (kcal/mol)
Co-crystalized ligand (641)	-7.017	0.847	N 13 O 15	O 0	HOH 743 (A) HTYR158 (A)	H-donor H-acceptor	2.91 3.13	-2.7 -1.2
A1	-6.860	1.248	C 6 -0.4	SD	MET199 (A)	H-donor	3.98	-0.8
A2	-6.465	1.532	N 12 O 8 O 15	O N NZ	ASP 148 (A) ILE 21 (A) LYS 165 (A)	H-donor H-acceptor H-acceptor	3.04 3.44 2.77	-1.1 -0.7 -3.1
A3	-7.167	1.750	C 6 N 12 N 20 O 21 5-ring	SD O SD O CB	MET 199 (A) ASP 148 (A) MET 199 (A) HOH 737 (A) BHE 149 (A)	H-Donor H-Donor H-Donor H-Acceptor Pi-H	3.62 2.99 4.28 2.85 4.16 -	-1.0 -2.0 -2.6 -0.9 -1.0
A4	-7.234	1.775	N 12 5-ring	O CB	ASP148 (A) PHE 149 (A)	H-donor pi-H	2.95 4.16	-1.5 -1.1
A5	-7.154	1.017	N 20 C 24 O 15 5-ring	O O CA CB	HOH 743 (A) PRO 156 (A) PRO 193 (A) PHE 149 (A)	H-donor H-donor H-acceptor pi-H	2.97 3.33 3.26 4.14	-3.7 -0.8 -0.9 -0.8

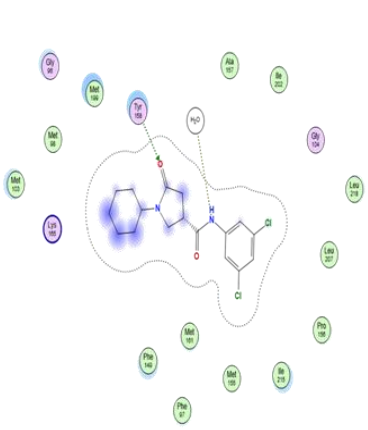

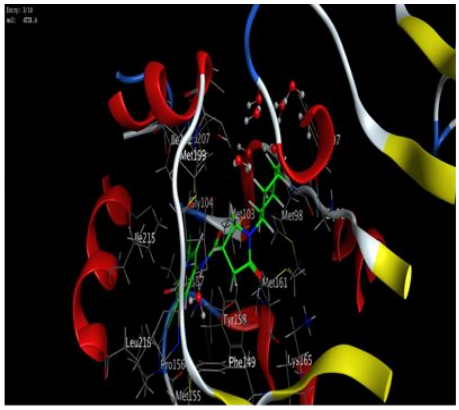

641

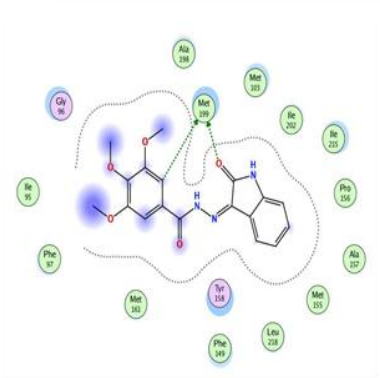

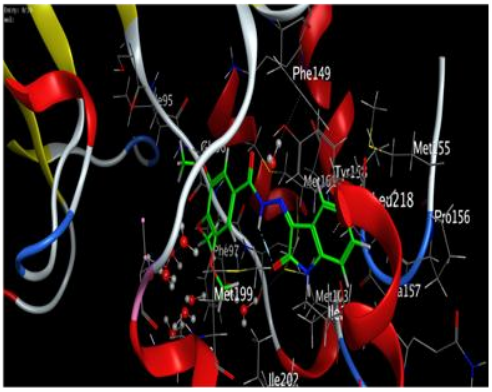

A1

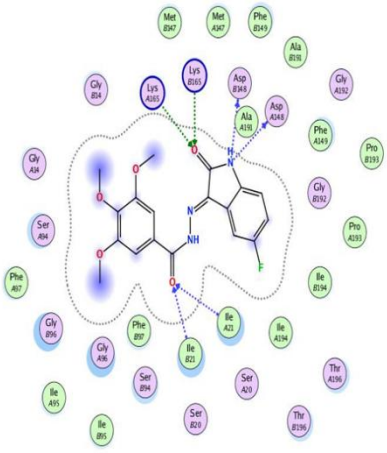

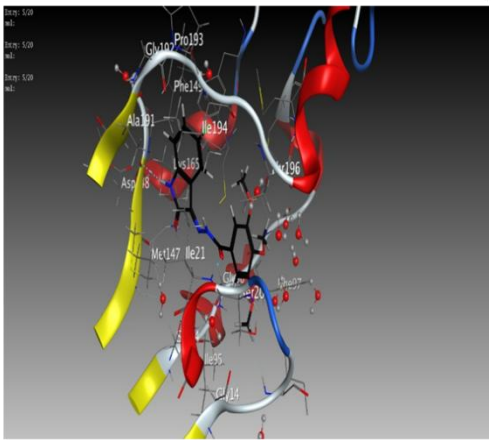

A2

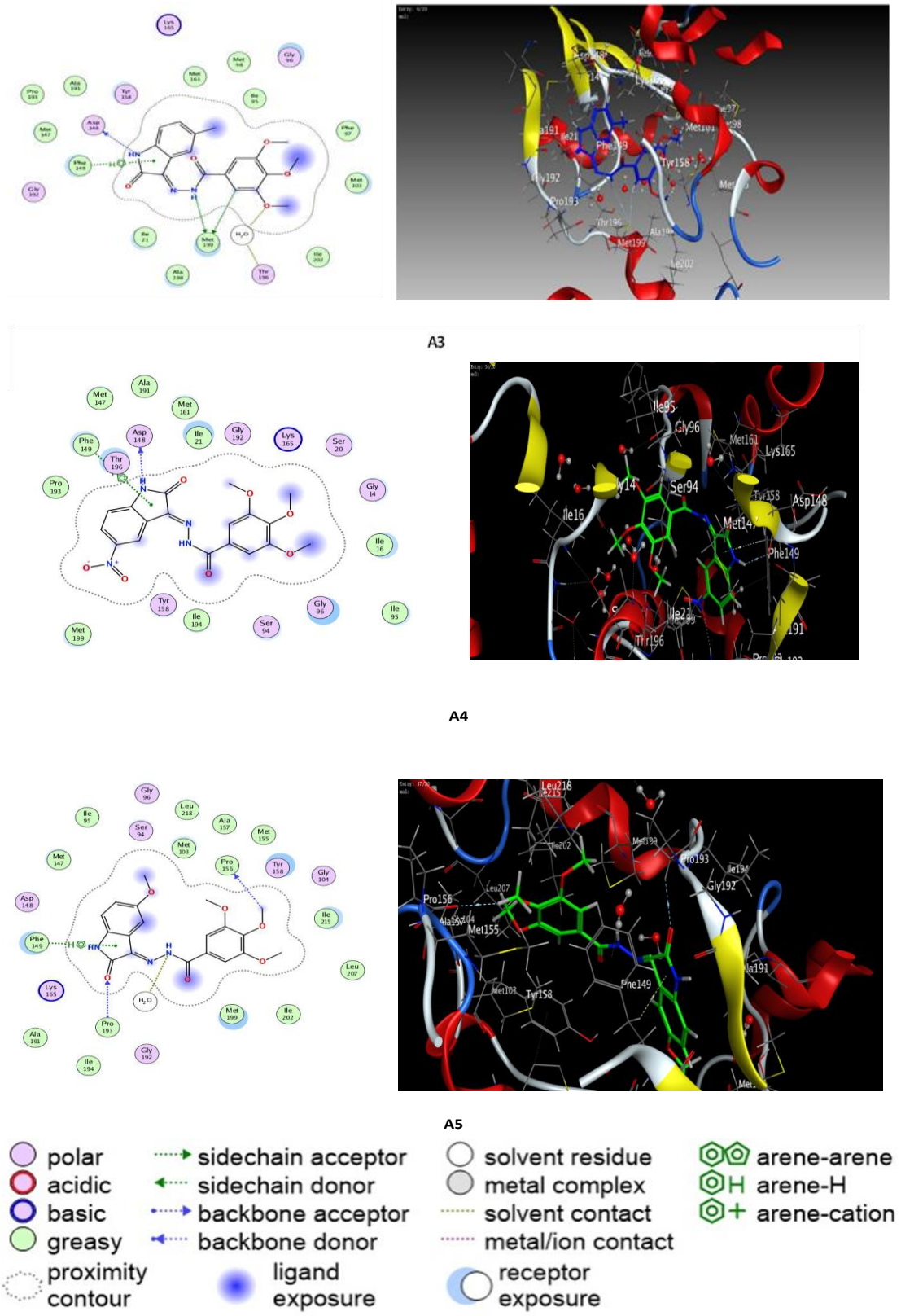

Figure2: Two-Dimensional (2D) and Three-Dimensional (3D) Interaction Diagrams of The Ligands Within the Active Site of **4TZK**.

4.Discussion

Molecular docking was conducted to evaluate the binding affinity and interaction of the synthesized isatin-based Schiff base derivatives **(A1–A5)** with the Mycobacterium tuberculosis (PDB ID: 4TZK), a key enzyme in the fatty acid synthesis pathway(Saeed and Al-Hamashi, 2023, Berman et al., 2000) **.** The Molecular Operating Environment (MOE) software was employed, using a rigid receptor approach and selecting the active site based on the co-crystallized ligand(Berman et al., 2000). All ligands were energy-minimized using the AMBER forcefield, and their 3D conformations were optimized prior to docking(Barillari et al., 2007).

The docking results revealed that all five ligands exhibited strong binding affinities within the active site of InhA, supported by favorable S-scores ranging from –6.8 to –8.3. These values indicate substantial binding potential, with ligands **A3** and **A5** demonstrating the most promising interactions. Notably, ligand **A5** exhibited the strongest binding affinity, which may be attributed to the presence of electron-withdrawing halogen substituents enhancing hydrogen bonding and hydrophobic interactions(Barillari et al., 2007, Inc, 2019). Key residues such as Tyr158, Ser94, Met103, and Phe149 were consistently involved in ligand binding across several compounds(Khan et al., 2018).In particular, ligands **A2** and **A4** also displayed stable docking poses through π–π stacking and hydrogen bonding, reinforcing their favorable orientation within the catalytic pocket(Meng et al., 2011)**.**Visual inspection of docking poses showed that the ligands were properly positioned, forming essential contacts necessary for enzyme inhibition (Pagadala et al., 2017)**.** Although RMSD was not prioritized due to the novelty of the ligands, the docking profiles were consistent and structurally reasonable (Priyanka Banerjee et al., 2018)**.** These results align well with ADMET predictions and biological activity forecasting via the PASS model, which suggested acceptable pharmacokinetic profiles and antitubercular potential **(Yadav et al., 2021)**. The findings support the hypothesis that isatin-based, when rationally modified, can effectively modulate binding interactions and orientation **(Зайков et al., 2024)**. Therefore, these derivatives-particularly ligand **A5**-hold promise as lead candidates for further in vitro and in vivo investigations in the development of new treatments against drug-resistant tuberculosis(Khan and Akhtar, 2022) **.**

5. Conclusion

Conclusion and Significance: The docking results predict that the isatin Schiff base derivatives (**A1-A5)** are promising inhibitors of M. tuberculosis enoyl reductase (4TZK), with binding affinities rivaling or slightly exceeding the co-crystallized ligand **(641)**. Key interacting residues identified include MET199, ASP148, LYS165, and PHE149. Although their predicted binding geometries (higher RMSD) differ more from the initial pose than the co-crystallized ligand **(641)**, they engage in more diverse and numerous interactions, including crucial H-bonds with ASP148/LYS165 and pi-H interactions with PHE149. Ligands **A3** and **A4**, exhibiting the strongest predicted binding energies (-7.167 and -7.234 kcal/mol), emerge as particularly noteworthy candidates for further investigation as potential anti-tubercular agents.

6. Acknowledgments

The authors are grateful to the University of Kufa for technical support and facilities.

References

ADENIJI, S. E., UBA, S. & UZAIRU, A. 2020. Multi-linear regression model, molecular binding interactions and ligand-based design of some prominent compounds against Mycobacterium tuberculosis. *Network Modeling Analysis in Health Informatics and Bioinformatics,* 9**,** 8.

BANERJEE, P., ECKERT, A. O., SCHREY, A. K. & PREISSNER, R. 2018. ProTox-II: a webserver for the prediction of toxicity of chemicals. *Nucleic acids research,* 46**,** W257-W263.

BARILLARI, C., TAYLOR, J., VINER, R. & ESSEX, J. W. 2007. Classification of water molecules in protein binding sites. *Journal of the American Chemical Society,* 129**,** 2577-2587.

BERMAN, H. M., WESTBROOK, J., FENG, Z., GILLILAND, G., BHAT, T. N., WEISSIG, H., SHINDYALOV, I. N. & BOURNE, P. E. 2000. The protein data bank. *Nucleic acids research,* 28**,** 235-242.

CASE, D. A., AKTULGA, H. M., BELFON, K., CERUTTI, D. S., CISNEROS, G. A., CRUZEIRO, V. W. D., FOROUZESH, N., GIESE, T. J., GOTZ, A. W. & GOHLKE, H. 2023. AmberTools. *Journal of chemical information and modeling,* 63**,** 6183-6191.

CHOWDHARY, S., SHALINI, ARORA, A. & KUMAR, V. 2022. A mini review on isatin, an anticancer scaffold with potential activities against neglected tropical diseases (NTDs). *Pharmaceuticals,* 15**,** 536.

FURNISS, B. S. 2004. *Practical organic chemistry*, Pearson Education India.

HAMADA, Y. & KISO, Y. 2017. Discovery of BACE1 Inhibitors for the Treatment of Alzheimer's Disease. *Quantitative Structure-Activity Relationship*.

HOSSAIN, S. & ZAKARIA, C. 2017. Structural and biological activity studies on metal complexes containing thiosemicarbzone and isatin based schiff base: a review. *Asian Journal of Research in Chemistry,* 10**,** 6-13.

HUSSEIN, S. A. A., MAHMOOD, A. A. R., TAHTAMOUNI, L. H., SALEH, K. M. M., RAMMAHA, M. S. & RIDHA, D. M. 2023. Synthesis, docking study, and cytotoxicity evaluation of new hydroxy benzoic acid derivatives. *Tikrit Journal of Pharmaceutical Sciences,* 17**,** 30-45.

INC, C. 2019. Molecular operating environment (MOE) version 2019.0102. *Montreal: Chemical Computing Group Inc*.

KHAN, S. A. & AKHTAR, M. J. 2022. Structural modification and strategies for the enhanced doxorubicin drug delivery. *Bioorganic Chemistry,* 120**,** 105599.

KHAN, T., LAWRENCE, A. J., AZAD, I., RAZA, S. & KHAN, A. R. 2018. Molecular docking simulation with special reference to flexible docking approach. *JSM Chem,* 6**,** 1053-1057.

KHATTAK, M., REHMAN, A. U., MUQADDAS, T., HUSSAIN, R., RASOOL, M. F., SALEEM, Z., ALMALKI, M. S., ALTURKISTANI, S. A., FIRASH, S. Z. & ALZAHRANI, O. M. 2024. Tuberculosis (TB) treatment challenges in TB-diabetes comorbid patients: a systematic review and meta-analysis. *Annals of medicine,* 56**,** 2313683.

LAGUNIN, A., STEPANCHIKOVA, A., FILIMONOV, D. & POROIKOV, V. 2000. PASS: prediction of activity spectra for biologically active substances. *Bioinformatics,* 16**,** 747-748.

MENG, X.-Y., ZHANG, H.-X., MEZEI, M. & CUI, M. 2011. Molecular docking: a powerful approach for structure-based drug discovery. *Current computer-aided drug design,* 7**,** 146-157.

NAZIR, H. & NASEER, M. M. 2025. The Isatin Scaffold: Exceptional Potential for the Design of Potent Bioactive Molecules. *Synlett*.

NYANG'WA, B.-T., BERRY, C., KAZOUNIS, E., MOTTA, I., PARPIEVA, N., TIGAY, Z., MOODLIAR, R., DODD, M., SOLODOVNIKOVA, V. & LIVERKO, I. 2024. Short oral regimens for pulmonary rifampicin-resistant tuberculosis (TB-PRACTECAL): an open-label, randomised, controlled, phase 2B-3, multi-arm, multicentre, non-inferiority trial. *The Lancet Respiratory Medicine,* 12**,** 117-128.

PAGADALA, N. S., SYED, K. & TUSZYNSKI, J. 2017. Software for molecular docking: a review. *Biophysical reviews,* 9**,** 91-102.

PAL, R., PANDEY, P., CHAWRA, H. S. & SINGH, R. P. 2025. Niosomal as Potential Vesicular Drug Nano-carriers for the Treatment of Tuberculosis (TB). *Nanoscience & Nanotechnology-Asia,* 15**,** E22106812323829.

PATEL, V. P., TRIPATHI, R. K. P. & DHARAMSI, A. 2025. Computational Exploration of Isatin Derivatives for InhA Inhibition in Tuberculosis: Molecular Docking, MD Simulations and ADMET Insights. *Current Computer-Aided Drug Design,* 21**,** 226-254.

PIRES, D. E., BLUNDELL, T. L. & ASCHER, D. B. 2015. pkCSM: predicting small-molecule pharmacokinetic and toxicity properties using graph-based signatures. *Journal of medicinal chemistry,* 58**,** 4066-4072.

PRIYANKA BANERJEE, P. B., ECKERT, A., SCHREY, A. & PREISSNER, R. 2018. ProTox-II: a webserver for the prediction of toxicity of chemicals.

REVUELTA-MAZA, M. Á., GONZÁLEZ-JIMÉNEZ, P., HALLY, C., AGUT, M., NONELL, S., DE LA TORRE, G. & TORRES, T. 2020. Fluorine-substituted tetracationic ABAB-phthalocyanines for efficient photodynamic inactivation of Gram-positive and Gram-negative bacteria. *European Journal of Medicinal Chemistry,* 187**,** 111957.

SAEED, A. M. & AL-HAMASHI, A. A. A. 2023. Molecular docking, ADMET study, synthesis, characterization and preliminary antiproliferative activity of potential histone deacetylase inhibitors with isoxazole as new zinc binding group. *Iraqi Journal of Pharmaceutical Sciences,* 32**,** 188-203.

THORAT, S. A., KANG, D. W., RYU, H., KIM, M. S., KIM, H. S., ANN, J., HA, T., KIM, S.-E., SON, K. & CHOI, S. 2013. 2-(3-Fluoro-4-methylsulfonylaminophenyl) propanamides as potent TRPV1 antagonists: Structure activity relationships of the 2-oxy pyridine C-region. *European journal of medicinal chemistry,* 64**,** 589-602.

YADAV, R., IMRAN, M., DHAMIJA, P., CHAURASIA, D. K. & HANDU, S. 2021. Virtual screening, ADMET prediction and dynamics simulation of potential compounds targeting the main protease of SARS-CoV-2. *Journal of Biomolecular Structure and Dynamics,* 39**,** 6617-6632.

ЗАЙКОВ, Х., ЗАМТИКОВА, М., МИХАЛЕВ, К., ИЛИЕВ, И. & ГЕОРГИЕВА, С. 2024. ISATIN AND ITS DERIVATIVES: REVIEW OF PHARMACOLOGICAL ACTIVITIES AND THERAPEUTIC POTENTIAL. *Management & Education/Upravlenie i Obrazovanie,* 20.